Optimizing Sparse Allocation for Radar Spectrum Sharing

Peng Seng Tan, James M. Stiles and Shannon D. Blunt
Radar Systems Lab, University of Kansas, Lawrence, KS

***Abstract*— Increasing demand by wireless communication applications for spectrum bands predominately occupied by radar applications has led to challenging resource allocation issues in the congested spectrum environment. A new resource allocation scheme based on Marginal Fisher's Information (MFI), is proposed to address the issue of spectrum congestion. Using MFI, which in some cases is identical to integrated sidelobe level (ISL), as the optimization metric, a Sparse Spectrum Allocation algorithm is shown to optimally reallocate a sparse bandwidth while ensuring range resolution performance is maintained and minimizing the degradation in sidelobe performance**

Keywords—component; formatting; style; styling; insert (*key words****)***

I. INTRODUCTION

The ever increasing demand for RF spectrum by the wireless communication industry has resulted in the push towards several major research directions, such as investigation of the performance degradation between radar and wireless communications when both systems are coexisting in operations [1,2]. In addition, there are efforts to develop sophisticated radar waveforms that are either spectrally well contained [3,4] or able to support joint radar/wireless communications systems operating within the same spectrum band [5-7]. Some recent examples of waveforms that support joint operations of both systems are multi-modal OFDM waveforms or sparse frequency waveform designs. Note that sparse frequency waveform design can also be viewed as thinned spectrum waveform design [8]. In this paper, we consider the problem of spectrum congestion/sharing from an information theoretic perspective.

Consider a contiguous RF spectrum band as consisting of many distinct spectral lines as in a line spectrum represented in optical spectroscopy [9]. Using this analogy, the contiguous spectrum band can be defined by the generic expression

$$\mathbf{s}(w)=\sum_{n=1}^{N} s_n \delta(w-w_n). \qquad (1)$$

In the above expression, $s(w)$ represents the original contiguous spectrum that has been defined to consist of a summation of N spectral lines with each spectral line defined by a Dirac-Delta function $\delta(w)$ offset at the frequency location w_n and weighted by the value s_n. When applied to a pulsed radar system transmitting at the pulse repetition frequency of w_{PRF}, the expression will be altered to that of

$$\mathbf{s}(w)=\sum_{n=1}^{N} s_n \delta(w-nw_{PRF}). \qquad (2)$$

By examining the above equation, it can be seen that in a pulsed radar system, not all the frequency content are utilized in the given contiguous spectral band as each spectral line is separated by the PRF interval. As such, there arises the question of whether the radar needs the full contiguous spectrum in order to achieve the desired range resolution. If not, then there exists the possibility of removing some of these spectral lines within the band in an optimal manner without having to degrade the range resolution, i.e. a form of spectral thinning. Meanwhile, the remaining spectral lines do not necessary have to be placed at frequency locations that are integer multiples of the PRF value but can be any frequency interval so long as this interval is lower than the PRF value so as to avoid range ambiguity. This effect will be analogous to the application of PRI jittering in pulse radar [10]. Also, this approach is realizable if we first consider each i^{th} spectral line located at frequency w_i to represent an individual narrowband coherent transmitter/receiver. Subsequently, during each pulse repetition interval (PRI), all the coherent transmitters emit simultaneously at their assigned frequencies for a pre-defined duty cycle within the PRI. As the effective bandwidth is maintained by jointly processing the returns from all receivers over an interval of time, range resolution is maintained as well.

Thus, by using the above representation, the whole contiguous band can also be analogous to a uniform-spaced linear (ULA) antenna array in which each spectral line corresponds to an array element. This perspective then opens the possibility to apply techniques developed for antenna array thinning into the spectrum thinning problem mentioned above. For instance, we can now view the problem from the perspective of allocating minimal frequency content while maintaining the range resolution for minimal sidelobe degradation. This viewpoint is analogous to the concept of the minimum redundancy linear array (MRLA) [11] within the antenna array community.

Previous research on generating MRLA can be grouped into two categories, i.e. either non-statistical or statistical approaches. For the non-statistical approach, some examples are such as those reported in [11-14] that are variant adaptations to the findings on deriving both unrestricted and restricted difference bases of integers as reported by Leech [15]. For the statistical approach, the results are generated using either Pattern Search algorithms [16], Particle Swarm Optimization [17] or the Genetic Algorithm [18] among others. However, one limitation common to all these approaches is the

ability to produce the MRLA or at least, a low redundancy linear array (LRLA) when the original array size to be thinned is large, i.e. consisting of hundreds of array elements or more. Furthermore, the algorithms used in the statistical approach also require large computation time to generate results for any sizable array dimension. To overcome these limitations using the above approaches, an alternative algorithm that is based on a measure known as the Marginal Fisher's Information (MFI) [19] was derived for generating a large sparse array configuration with minimum or low redundancies in the coarray while using much less computational resources as compared to the statistical approach. Here, this approach is proposed to perform the optimal selection of spectral lines within the full spectrum band while ensuring that the range resolution performance is maintained.

II. PROBLEM FORMULATION

A. Radar Measurement Model

As described in the previous section, it is possible to view the contiguous RF spectrum for a radar system to be consisting of many spectral lines with each spectral line representing a physical coherent transmitter that transmits a waveform with constant amplitude at a frequency that corresponds to that spectral line. Also, the transmitter will be turned on/off with a finite duration during each period corresponding to the PRI. Thus, it is possible to define a radar measurement model in the frequency domain as in the time domain. For a start, we define the measurements received at the radar over the CPI duration by the following equation

$$\mathbf{v} = \mathbf{H}\boldsymbol{\gamma} \tag{3}$$

$$\mathbf{H} = [\mathbf{h}_1, \mathbf{h}_2, \mathbf{h}_i, \ldots.], i = 1 \ldots . M \ , \tag{4}$$

where the symbol $\mathbf{v}$ is a Kx1 radar measurement vector in frequency, $\mathbf{H}$ is a KxM matrix that is the observation matrix for this model. Note that for the matrix $\mathbf{H}$, each element along the row dimension represents an observation associated with a unique and increasing frequency and each element along the column dimension represents an observation associated with a unique and increasing target distance from the radar receiver. Thus, $\mathbf{H}$ can also be represented by M column vectors $\mathbf{h}_i$ as shown in (4). Also, an analogy to the column vector $\mathbf{h}_i$ in (4) will be the array manifold vector corresponding to the physical angle θ_i in a direction finding problem. Finally, $\boldsymbol{\gamma}$ is an Mx1 vector with each element γ_i corresponding to the complex scattering coefficient of a target located at distance $\mathbf{x}$ meters away from the radar receiver.

Before going further, it must be emphasized that taking measurement samples in frequency is the dual problem of taking measurement samples in time. As it is well known that the temporal sampling rate will determine the sampling bandwidth in frequency, thus the corresponding frequency sampling interval between two frequency samples will also determine the temporal timespan in time corresponding to unambiguous target distance. At the same time, while the total observation time T_0 for temporal sampling determines the frequency resolution (1/ T_0), so will the span of the frequency samples determines the temporal resolution, i.e. range cell resolution in meters.

Going further, (3) is further modified to include the complex measurement noise vector $\mathbf{n}$ such that the final radar measurement model in frequency is as follows

$$\mathbf{v} = \mathbf{H}\boldsymbol{\gamma} + \mathbf{n} \ . \tag{5}$$

This form of this equation is what is popularly known in literature as the linear model. An additional note to take is that as there is a one-to-one mapping between the target distance $\mathbf{x}$ with the time delay τ_d to the receiver, the elements in vector $\boldsymbol{\gamma}$ can be viewed as a Target Delay Spectrum of the time delay parameter τ_d .

B. Cramer Rao Bound and Marginal Fisher Information

By defining the radar measurements in frequency as a linear model given in (5), we can then proceed to examine the relationship between the amount of frequency measurements allocated in $\mathbf{v}$ with that of the estimation of the vector $\boldsymbol{\gamma}$ which we will denoted by the symbol $\tilde{\gamma}$. Now, the estimation error and its corresponding covariance matrix given by the following:

$$\boldsymbol{\varepsilon} = \tilde{\boldsymbol{\gamma}} - \boldsymbol{\gamma} \tag{6}$$

$$\mathbf{K}_{\varepsilon} = E\{\boldsymbol{\varepsilon}\boldsymbol{\varepsilon}'\} \ . \tag{7}$$

From [20], it is known that the lower bound of the error covariance is given by the Cramer-Rao Lower Bound (CRLB) which is equal the inverse of the Fisher Information of the measurement vector. At the same time, for the linear model defined in (5), when applying an efficient estimator such as the Minimum Mean Square Error (MMSE) estimator to the measurements, the error covariance obtained for the estimated $\tilde{\gamma}$ will be equal to the CRLB. Thus, it is with this understanding, that the algorithm based on the Marginal Fisher Information (MFI) is then derived. For instance, if we denote the Fisher Information matrix from the K number of measurements in $\mathbf{v}$ as $\mathbf{J}_{\mathbf{K}}$, and the Fisher Information matrix of the (K-1) measurements that excludes the k^{th} measurement located at w_j as $\mathbf{J}_{\mathbf{K\text{-}1}}$, the MFI of this k^{th} measurement is defined as the nonnegative definite matrix $\Delta\mathbf{J}(K)$ expressed as

$$\Delta\mathbf{J}(K) = \mathbf{J}_{\mathbf{K\text{-}1}}^{-1} - \mathbf{J}_{\mathbf{K}}^{-1} \ . \tag{8}$$

In a way, the MFI is a measure of the new information that is obtained by adding the k^{th} measurement to the original (K-1) measurements. From the perspective of sparse array design, the MFI can also be viewed as a "reduction in uncertainty" metric since adding the k^{th} measurement will either leave the matrix $\Delta\mathbf{J}(K)$ unchanged when compared to matrix $\Delta\mathbf{J}(K\text{-}1)$ that correspond to (K-1) measurements or reduce the error variances of the estimated $\tilde{\boldsymbol{\gamma}}$ based on the additional information provided by the k^{th} measurement. However, from the perspective of array thinning starting from an initially fully filled array, the MFI can be viewed as the amount of increase

in the error variances of $\tilde{\boldsymbol{\gamma}}$ when the number of measurements in the vector $\mathbf{v}$ has been reduced by one from the initial K number of measurements. Finally, to complete the problem formulation, the Fisher Information matrix $\mathbf{J_K}$ is defined as

$$\mathbf{J}_K = \left(\mathbf{H}'\mathbf{K}_\mathbf{n}^{-1}\mathbf{H} + \mathbf{K}_\gamma^{-1}\right) \quad (9)$$

where $\mathbf{K_n}$ is the covariance matrix due to the measurement noise and is defined by the following equation

$$\mathbf{K_n} = E\{\mathbf{nn}'\} = \sigma_n^2\mathbf{I}. \quad (10)$$

Also, $\mathbf{K}_\gamma$ is the a priori target covariance matrix and is defined by the following equation

$$\mathbf{K}_\gamma = E\{\boldsymbol{\gamma\gamma}'\} = \sigma_\gamma^2\mathbf{I}. \quad (11)$$

With the above definition, (9) can then be rewritten as

$$\mathbf{J_K} = \left(\sigma_n^{-2}\mathbf{H}'\mathbf{H} + \sigma_\gamma^{-2}\mathbf{I}\right). \quad (12)$$

C. Optimal Spectrum Band allocation based on MFI

For this paper, we will be adopting the first perspective of sparse array design when we are using the MFI metric to design the algorithm to allocate the optimal locations for a K number of spectral lines out of a N number of total spectral lines where $N > K$. Initially, we will place the location of the first frequency measurement sample corresponding to the first spectral line, i.e. $-BW/2$ where BW is the span of the contiguous spectrum band. Subsequently, we will use the MFI metric to determine the optimal spectral locations of the 2nd to the K^{th} frequency measurement sample using a greedy search method on a sample by sample increment basis. Note that the location of the $(M+1)^{th}$ measurement that is added to a frequency array of M measurements is based on the candidate out of $(N\text{-}M)$ possibilities that produces the largest reduction of the estimation error. After all the initial K frequency locations have been allocated, the iteration is then repeated until the results have reached convergence.

III. SIMULATION AND RESULTS

In order to evaluate the performance of the proposed sparse spectrum allocation algorithm described in the previous section, the following simulation scenario assumed for a radar application is set up in MATLAB with the parameters as shown in Table 1 as follows.

TABLE I. SIMULATION PARAMETERS

Parameter type	Parameter value
Span of N frequency samples, $\boldsymbol{BW}$	-10 kHz to 10 kHz
Unambiguous target range/delay $\boldsymbol{T_0}$	0.01 second
Nyquist sampling requirement for $\boldsymbol{T_0}$; $2 * T_0$	0.02 second
Nyquist frequency sampling interval, $\boldsymbol{F_s}$	$\frac{1}{2 * T_0} = 50\,Hz$
Sampling grid for frequency samples	5 Hz
Total number of frequency samples required for BW under Nyquist, $\boldsymbol{N}$	$\frac{BW}{F_s} = 400$
Number of selected samples, $\boldsymbol{K}$	100 (25%)
Target variance σ_γ^2	1.00
Noise variance σ_n^2	1.00

Now, for this simulation, instead of assuming that every spectral line represents an individual narrow-band coherent transmitter/receiver as was stated in Introduction section, it is now assumed that each line is just a frequency tone with zero bandwidth for simplicity sake. At the same time, note that the intent of the fine sample grid size of 5 Hz is meant to introduce more degrees of freedom for the MFI allocation algorithm in placing the locations of the K spectral lines so that the spacing between any two spectral lines does not have to be an integer multiple of the Nyquist sampling interval F_s.

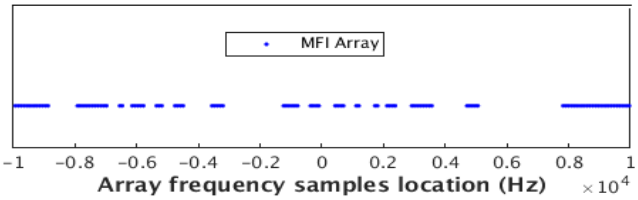

Figure 1. Frequency sample locations for MFI generated array for K = 100 (25% of total bandwidth)

As a start, the plot showing the frequency sample locations for K = 100 samples (25% utilization of total bandwidth) obtained using the MFI based algorithm is shown in Figure 1 above. By examining this figure analytically, the first observation is that the minimum frequency spacing between samples is equal to 80 Hz which is lower than 100 Hz corresponding to the unambiguous target range delay T_0. Also, there is no fixed periodicity present in the frequency spacing between these 100 frequency samples. The next observation made is that there are various gaps of unequal sizes in the array with the two largest gaps having widths of 2765 Hz and 1900 Hz respectively. Now, the presence of these gaps with unequal width seems to indicate that the allocation algorithm determines that the irregular spacing between the samples will produce the least possible error variances in estimating $\boldsymbol{\gamma}$ when using just 100 frequency measurement samples as compared to uniform spacing. Likewise, from the perspective of measurement redundancies, the algorithm determines that the irregular spacing will produce an array with lower redundancies in its coarray as compared to using uniformly-spaced frequency.

This deduction based on the second observation is validated by examining the plot of the coarray from the MFI generated array with that of the uniformly-spaced frequency array as show in Fig. 2. From the plot, we can see that the MFI generated array does generate a coarray with much lower redundancies that resembles a LRLA as compared to the

uniformly-spaced frequency array that contains high redundancy values.

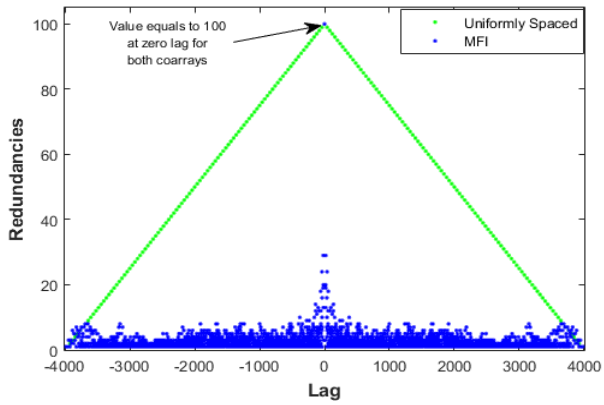

Figure 2. Coarrays from MFI generated array and uniformly-spaced frequency array using $K = 100$ for both arrays

Next, in order to examine the estimation error variances that will arise when using this array, the Matched Filter operation is applied to compute the estimation errors that will arise when estimating the target located at the start of the unambiguous target range, i.e. at 0 delay. The resulting plot obtained is analogous to the beam pattern obtained when using the Delay-Sum beamformer as the weight vector in array beamforming operation.

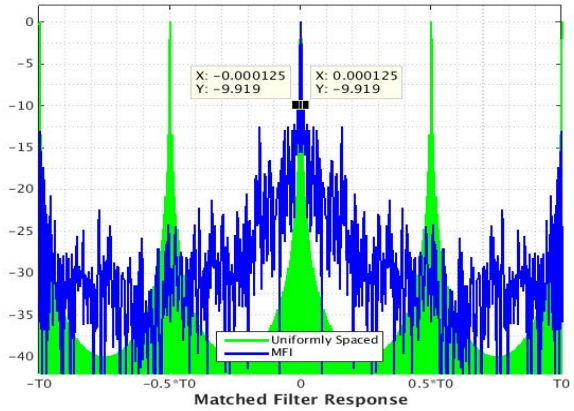

Figure 3. Matched Filter Response using MFI generated array for $K = 100$

From Fig. 3 above, the first observation is that the sidelobe levels obtained from the MFI generated frequency measurement array are generally lower than -10.0 dB with the exception of two peak sidelobes having a value of -9.92 dB near to the main lobe. This means that if there is a target with non-zero γ value located at the range corresponding to ±0.000125 second delay in the range profile, it will contribute maximum error to the estimation of the γ value located at 0.00 second delay. The second observation made is that there is no grating lobe present within the unambiguous range when using the MFI generated array. The reason is because there is no fixed periodicity in the spacing between samples in the MFI generated array. Thus, although the sidelobe performance of the uniformly-spaced frequency array are much better than that of the MFI generated array for the same $K = 100$ measurements, grating lobes will appear within the span of T_0 due to the spacing between samples is greater than 100 Hz corresponding to T_0.

Having observed the superior performance of the MFI generated array to that of the uniform-spaced array for $K = 100$, we also compare this sparse array to that of an array of the same size whose K locations are randomly generated by using a random permutation of all possible frequency locations. Next, we plot the result of the ISL of the MFI generated array versus that of the histogram results obtained from 10000 trials of randomly-spaced array.

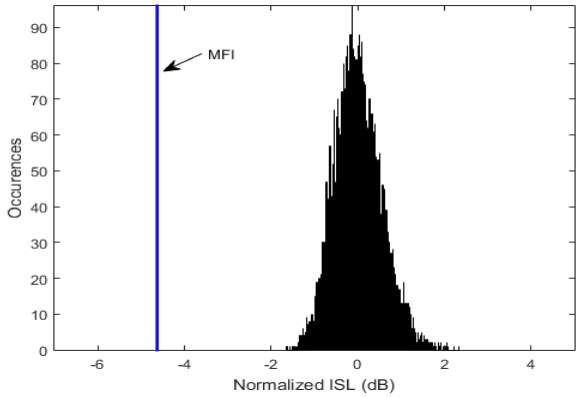

Figure 4. ISL value from MFI generated array and randomly-spaced frequency array using $K = 100$ and 10000 trials

From Fig. 4 above, the computation of the normalized ISL from the randomly-spaced frequency array has a standard deviation of 0.5299 dB. Compared to the ISL result from the MFI generated array whose value is -4.636 dB, this shows that the result from the Sparse Spectrum Allocation algorithm (MFI based) is 8.7492 standard deviations away from the average value of the randomly-spaced array. Thus, it can be seen that it is virtually impossible to generate the result obtained using the MFI based algorithm via random permutation.

Next, we then consider the case when the bandwidth has doubled to 50%, i.e. $K = 200$ measurements and results of the coarray and the Matched Filter Response are shown in Fig. 5 and Fig. 6 respectively.

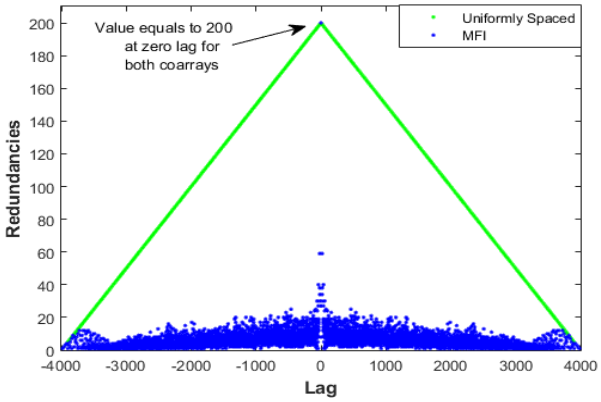

Figure 5. Coarrays from MFI generated array and uniformly-spaced frequency array using $K = 200$ for both arrays

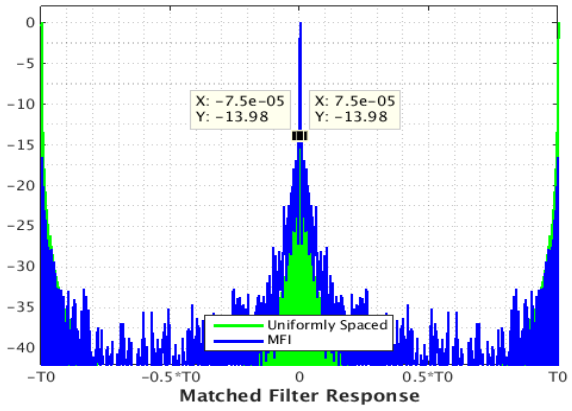

Figure 6. Matched Filter Response using MFI generated array for $K = 200$

By comparing the results as shown in Fig. 2 with that from Fig. 5, we can observe that the MFI generated array still generate a coarray with low redundancies that resembles a LRLA even when the number of frequency measurements have doubled to 200. Likewise from Fig. 6, we observe an improvement in the peak side-lobe performance from a value of -9.92 dB when $K = 100$ to a value of -13.98 dB when $K = 200$.

At this stage, based on the results obtained using the MFI-based sparse spectrum allocation algorithm, we have shown that it is possible to release spectral content from the radar application while maintaining the radar range resolution but at a cost of degraded ISL and PSL performance when compared to using the full contiguous spectrum band.

Next, in order to demonstrate the feasibility of using the results from this new sparse spectrum allocation scheme for radar applications, we will apply it to a simple radar target estimation problem for a simulated scenario at which there are a total of eight complex-valued targets that are sparsely located within the range profile (target delay spectrum) spanning T_0 second and containing a total of 200 range cells. Details and results of the target estimation problem are as described in the next section.

IV. ESTIMATION OF γ USING MFI GENERATED SAMPLING ARRAY

As mentioned in the previous section, a total of eight complex-valued targets that are sparsely located within the range profile are setup for the radar target estimation problem. As a start, each of these eight targets is assumed to be contained within one range cell as the focus is not on dealing with extended targets in this paper. Following that, the details of the locations and magnitude of the eight targets are provided in Table 2 below:

TABLE II. SIMULATION PARAMETERS

Target Number	Location (ms)	$\lvert\gamma_i\rvert$	Magnitude of $\lvert\gamma_i\rvert^2$ in dB
1	0.850	0.899	-0.924
2	2.650	1.000	0
3	4.500	0.475	-6.46
4	5.300	0.795	-1.998
5	6.450	0.499	-6.047
6	7.700	0.501	-6.003
7	9.350	0.3112	-10.139
8	9.550	0.3069	-10.261

Next, information of these eight sparsely distributed targets are first captured in a frequency measurement vector $\mathbf{v}$ of length 100 using the results of the MFI algorithm obtained for $K = 100$ samples for the frequency locations. At the same time, a complex-valued white Gaussian noise vector $\mathbf{n}$ of the same length 100 with a noise variance σ_n^2 of -20 dB w.r.t the target with largest γ_i is added to the measurement vector $\mathbf{v}$ so as to complete the linear model represented by (5) in section II.

For the target estimation implementation, firstly, we perform a target estimation operation by using the Matched Filter to estimate a first iteration estimate of all 200 target scattering coefficients in vector $\tilde{\gamma}$ within the target delay spectrum. Secondly, we then perform a threshold operation to identify the range cells corresponding to the elements from $\tilde{\gamma}_{\text{Matched}}$ that are greater than a predefined threshold value (choose as -12 dB from the magnitude of the largest element in $\tilde{\gamma}_{\text{Matched}}$ for this paper). Once this smaller subset of range cells is identified from the whole target profile of 200 range cells, the magnitude γ_i of all the remaining range cells are set to zero. Subsequently, we then perform a second target estimation operation using the MMSE filter to estimate the values of the smaller length target vector that we denoted as $\tilde{\gamma}_{\text{MMSE}}$. The final estimated values of the complex scattering coefficients for all 200 targets in the target delay spectrum is as shown in Fig 7 below.

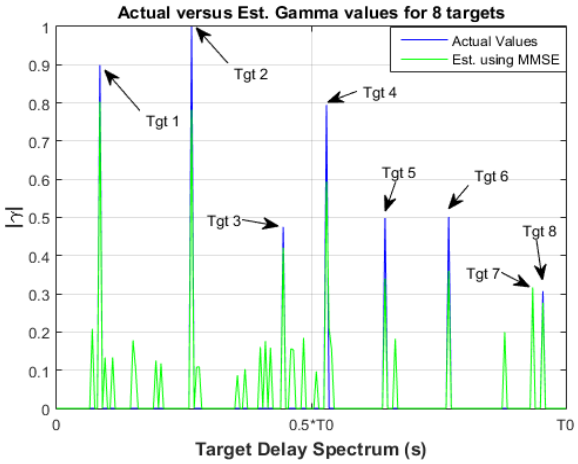

Figure 7. Actual versus Estimated $\tilde{\gamma}$ for $K = 100$

From the results shown in Fig. 7 above, it can be seen that by using a small number of frequency measurements (K = 100) corresponding to 25% of total bandwidth, the target estimation operation is able to estimate the values of the eight sparsely distributed complex-valued targets quite accurately along with some false alarms in other range cells. For this example, the error variance computed between the actual $\boldsymbol{\gamma}$ vector and the estimated $\tilde{\boldsymbol{\gamma}}$ by considering all 200 range cells within the range profile has a value of -6.767 dB.

Now, when the number of measurements has been doubled to 50% of the total available bandwidth (K = 200), besides improving the accuracy in estimating the values of the eight sparsely distributed complex-valued targets, the false alarms have also gone down significantly as shown in Fig. 8 below. For the 2nd example, the error variance computed between the actual $\boldsymbol{\gamma}$ and the estimated $\tilde{\boldsymbol{\gamma}}$ has improved to a value of -14.234 dB.

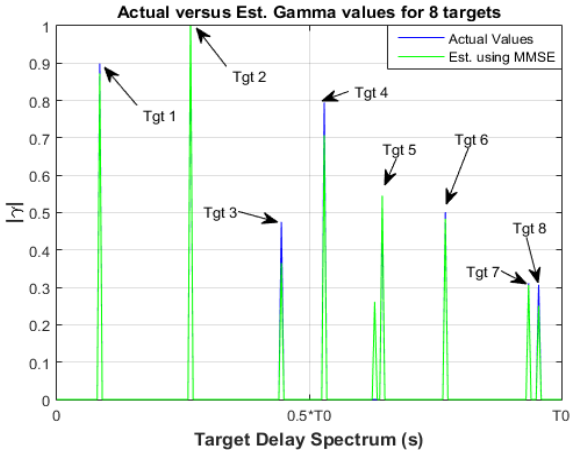

Figure 8. Actual versus Estimated $\tilde{\gamma}$ for K = 200

V. CONCLUSION

In this paper, we have attempted to directly address the core issue of Spectrum Congestion by introducing a novel approach to allocate a sparse/disjoint spectrum from an original contiguous spectrum to the radar system without causing any degradation to its performance in range resolution. The main mechanism behind this new approach is the use of the Marginal Fisher Information (MFI) as the optimization metric when allocating the sparse spectrum to the radar system. Finally, we have also demonstrated the viability of using the results of this new sparse spectrum allocation algorithm by applying these results to a simple radar target estimation problem.

REFERENCES

[1] M.R. Bell, N. Devroye, D. Erricolo, T. Koduri, S. Rao and D. Tuninetti, "Results on spectrum sharing between a radar and a communications system," in *Proc. Intl. Conf. on Electromagnetic Advanced Application*, Palm Beach, Aruba, Aug. 2014.

[2] H. Wang, J. Johnson, C. Baker, L. Ye, C. Zhang, "On spectrum sharing between communications and air traffic control radar systems", *IEEE Radar Conference*, May 2015.

[3] J. de Graff, H. Faust, J. Alatishe, and S. Talapatra, "Generation of spectrally confined transmitted radar waveforms: experimental results", *IEEE Radar Conference*, April 2006.

[4] S.D. Blunt, M. Cook, J. Jakabosky, J. de Graaf, and E. Perrins, "Polyphase-coded FM (PCFM) radar waveforms, part I: implementation," *IEEE Trans. Aerospace & Electronic Systems*, vol. 50, no. 3, pp. 2218-2229, July 2014.

[5] S. Gogineni, M. Rangaswamy, and A. Neho-rai, "Multi-modal OFDM waveform design," *IEEE Radar Conference*, April 2013.

[6] M. Lindenfeld, "Sparse frequency transmit-and-receive waveform design,", *IEEE Trans. Aerospace & Electronic Systems*, vol. 40, no. 3, pp. 851–861, 2004.

[7] G. Wang and Y. Lu, "Designing single/multiple sparse frequency waveforms with sidelobe constraint", *IET Radar, Sonar Navigation*, vol. 5, no. 1, pp. 32 –38, Jan. 2011.

[8] L.K. Patton, C.A. Bryant and B. Himed, "Radar-centric design of waveforms with disjoint spectral support," *IEEE Radar Conference*, May 2012.

[9] G. Gauglitz, D.S. Moore, *Handbook of Spectroscopy*, 2nd Enlarged edition, Wiley Online Library, 2014

[10] M.A. Richards, J.A. Scheer and W.A. Holm, *Principles of Modern Radar: Basic Principles*, SciTech Publishing, 2014

[11] A.T. Moffet, "Minimum-redundancy linear arrays," *IEEE Trans. Antennas &Propagation*, vol. 16, issue 2, pp. 172-175, Mar 1968

[12] K.A. Blanton and J.H. McClellan, "New search algorithm for minimum redundancy linear arrays," *International Conference on Acoustics, Speech, and Signal Processing*, vol .2, 1991.

[13] M.J. Rossouw, J. Joubert, and D.A. McNamara, "Thinned arrays using a modified minimum redundancy synthesis technique," *IET Electronic Letters*, vol. 33, no. 10, pp. 826–827, May 1997

[14] A. Camps, A. Cardama, D. Infantes, "Synthesis of large low-redundancy linear arrays", *IEEE Trans. Antennas & Propagation*, vol. 49, no. 12, , pp 1881-1883, Dec 2001.

[15] J. Leech, "On the representation of 1.2…n by differences," *J. London Math. Soc.*, vol. 31, pp. 160–169, April 1956.

[16] A. Razavi and K. Forooraghi, "Thinned arrays using pattern search algorithms", *Progress In Electromagn. Res.*,vol. 78, 2008

[17] M. Donelli, A. Martini, and A. Massa, "Square array based on Hadamard difference sets", *IEEE Trans. Antennas & Propagation*, vol. 57, no. 8, pp. 2491–2495, Aug. 2009

[18] J. Corcoles and M.A. Gonzalez, "Efficient combined array thinning and weighting for pattern synthesis with a nested optimization scheme", *IEEE Trans. Antennas & Propagation*, vol. 60, no. 11, pp. 5107–5117, Nov. 2012

[19] J.M. Stiles, J.D. Jenshank, "Spatial array construction using marginal fisher's information", *International waveform Diversity Conference*, Feb 2009

[20] S.M. Kay, *Fundamentals of Statistical Signal Processing: Estimation Theory*, 1st edition, vol 1., Prentice Hall, 1993.